Ammonia electrocatalytic synthesis from nitrate

Mini Review
doi.org/10.1002/elsa.202100220

Chemistry Europe
European Chemical Societies Publishing

Received: 30 December 2021
Revised: 30 March 2022
Accepted: 25 April 2022

Ammonia electrocatalytic synthesis from nitrate

Dimitra Anastasiadou[1,#] | **Yvette van Beek**[1,2,#] | **Emiel J. M. Hensen**[1] | **Marta Costa Figueiredo**[1,2]

[1]Laboratory of Inorganic Material and Catalysis, Department of Chemical Engineering and Chemistry, Eindhoven University of Technology, Eindhoven, The Netherlands

[2]Eindhoven Institute of Renewable Energy Systems (EIRES), Eindhoven University of Technology, Eindhoven, The Netherlands

Correspondence
Marta Costa Figueiredo, Laboratory of Inorganic Material and Catalysis, Department of Chemical Engineering and Chemistry, Eindhoven University of Technology, Eindhoven, The Netherlands.
Email: m.c.costa.figueiredo@tue.nl

[#]Dimitra Anastasiadou and Yvette van Beek contributed equally to the manuscript.

Funding information
Eindhoven Institute of renewable energy systems (EIRES)

Abstract

The interest in electrochemical processes to produce ammonia has increased in recent years. The motivation for this increase is the attempt to reduce the carbon emissions associated with its production, since ammonia is responsible for 1.8% of the global CO_2 emissions. Moreover, green ammonia is also seen as a possible transportation fuel in various renewable energy transition scenarios. Several electrochemical processes are being investigated such as N_2, NO_3^-, or NO conversion. Since nitrates are an attractive source of nitrogen, due to their role as water contaminants and facility to break N-O bonds, this mini review is focused on the electrocatalytic synthesis of ammonia from NO_3^- reduction. Here, we summarized the important work on reaction mechanisms and electrocatalysts for this reaction.

KEYWORDS
Ammonia, catalytic activity, electrochemical reduction, electrocatalyst, mechanism, nitrate, reaction pathway

1 | INTRODUCTION

Ammonia (NH_3) is a gas lighter than air (under 60% of the density of air) with a strong odor and is one of the most used chemicals in the world. It is mainly used to produce fertilizers, refrigerants, explosives, as well as textiles and pharmaceuticals, but further uses are expected to arise.[1] For example, NH_3 can be used as a transport fuel through combustion in an internal combustion engine or for electricity generation in alkaline or Proton exchange membrane fuel cells[2] (Figure 1). As such, it also represents a medium to store thermal or chemical energy.[3] NH_3 can also be decomposed to its elements, providing a good source of hydrogen (H_2). The volumetric H_2 energy density in liquid anhydrous NH_3 is significantly higher than that of liquid H_2 and compared to common liquid fuels (methanol, ethanol, gasoline, LPG) has the advantage of being carbon-free.[4] At ambient temperatures, NH_3 stays in liquid form above 9 bar, which makes its storage, transportation, and distribution relatively easy. Furthermore, safe handling procedures of large quantities of NH_3 are well established, along with the infrastructure for its transportation by pipelines, rails, and roads.[5]

Ammonia's commercial production was started by Haber and Bosch at the beginning of the 20th century. It is considered as one of the most important industrial processes ever developed, since it caused the world population to sprout. The annual NH_3 production based on

Mini Review
doi.org/10.1002/elsa.202100220
Chemistry Europe
European Chemical Societies Publishing

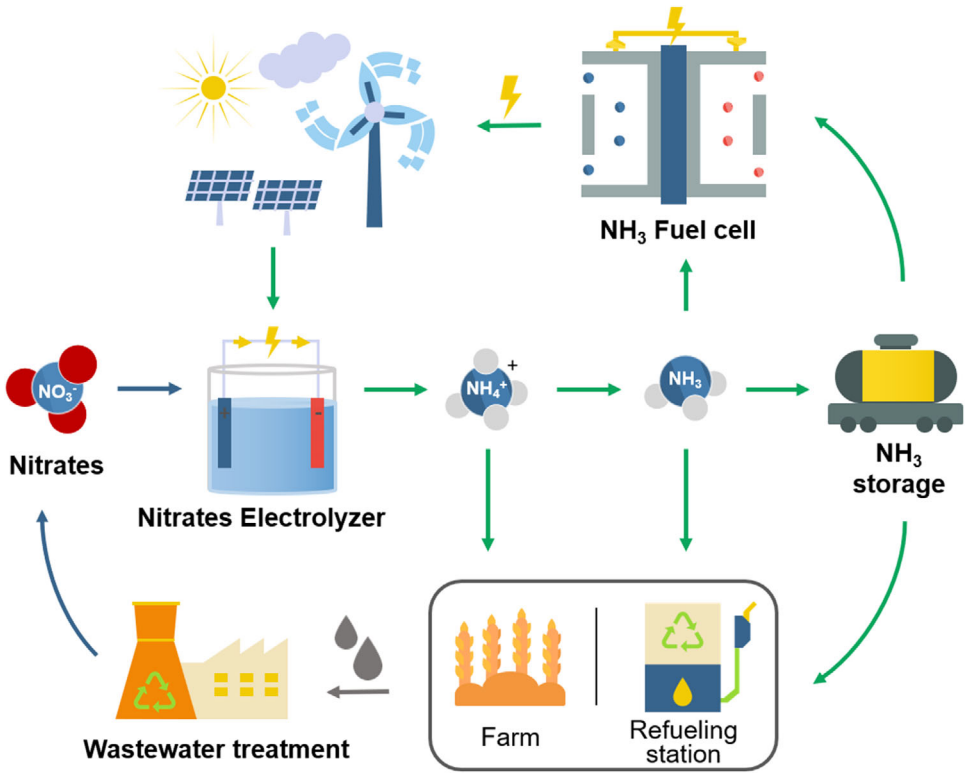

FIGURE 1 Concept for electrochemical ammonia synthesis from agricultural and industrial waste streams to create a closed *N*-cycle

Haber–Bosch is about 176 million tons[6] and due to a large number of applications and products where NH_3 is utilized, a production capacity growth of 1.2 billion metric tons is expected by 2050.[7] Haber–Bosch synthesis requires the reaction of H_2 and nitrogen (N_2) over typically iron-based catalysts at temperatures in the range of 500°C and pressure up to 300 bar. The H_2 used, is currently sourced from natural gas, which undergoes desulphurization, followed by methane steam reforming and water-gas shift reaction to convert carbon monoxide (CO) and H_2O to H_2 and carbon dioxide (CO_2).[8] This process is highly energy-intensive and consumes around 1.8% of the global yearly energy output, and produces 500 million tons of CO_2. NH_3 along with cement, steel, and the production of ethylene is one of the biggest carbon-emitting industrial processes.[3] Therefore, the need to decarbonize NH_3 production by less energy-intensive alternatives is currently being investigated.

Several electrochemical routes to synthesize NH_3 are currently under development.[9] For example, the H_2 required for the Haber–Bosch reaction can be sourced from water electrolysis.[9] In addition to providing green H_2, the use of water as a starting material would help to prevent catalyst poisoning from CO or sulfur compounds, which can be found in H_2 obtained from natural gas. An alternative electrochemical route that is under preliminary investigation is the direct NH_3 synthesis via the electrochemical reduction of N_2 or nitrate (NO_3^-).[1,10] Despite widespread interest, electrochemical reduction of N_2 is a great challenge.[11] The cleavage of the N_2 molecule requires the breaking of three bonds and, thus, needs substantial dissociation energy. This leads to high ovepotential for N_2 electroreduction, and favors H_2 evolution. The intermediates from H_2 evolution can also poison the surface and inhibit catalytic activity.[11] In this context, the direct electrosynthesis of NH_3 through NO_3^- presents some advantages. First, the amount of energy required to dissociate the $N = O$ bond is much less than for the $N \equiv N$ bond, that is, 607 kJ/mol compared to 941 kJ/mol, respectively.[12] Moreover, NO_3^- has nearly a 40,000-fold higher solubility in water than N_2[13] and its utilization as a source for NH_3 can help in decreasing NO_3^- contaminations in water. NO_3^- is a pollutant, commonly found in surface and groundwater due to geogenic and anthropogenic activities, like the manufacture of explosives, nuclear energy, and metal finishing industries.[14,15] These usages led to a significant increase in the NO_3^- concentration in drinking water in the last decades.[16] Excess of NO_3^- induces human health problems such as methemoglobinemia, clinical cyanosis (blue baby syndrome), and carcinogenic nitrosamines which are formed by the reduction of NO_3^- to nitrite (NO_2^-) in the human body.[15] Thus, the World Health Organization set a maximum of 50 mg/L NO_3^- in drinking water (3 mg/L for NO_2^-) to

Mini Review
doi.org/10.1002/elsa.202100220
Chemistry Europe
European Chemical Societies Publishing

avoid such health risks.[17] Furthermore, NO_3^- is accountable for other environmental issues like mineral depletion from the soil as well as increased acidity of downstream or coastal water.[18] Consequently, the removal of NO_3^- (and NO_2^-) from water has become important for public health. Several technologies have been implemented for this purpose including electrodialysis, reverse osmosis, ion exchange resins, and biological processes.[19] Unfortunately, these processes result in the formation of additional products and require extra processing steps.[20] Thus, electrochemical processes like NO_3^- reduction to NH_3 are promising, because they limit the formation of harmful byproducts while allowing the use of renewable energy. In this review, we will focus on NH_3 production via the electrochemical reduction reaction of NO_3^-.

2 | REACTION MECHANISM

The electrochemical production of NH_3 from NO_3^- follows an eight-electron transfer process, with oxidation states ranging from +5 in NO_3^- to -3 in NH_3.[21] Previous works[22–28] have shown that the electrochemical reduction of NO_3^- can result in the formation of several possible nitrogen species as products through different pathways (Figure 2). The preferred pathway depends on the electrocatalyst (and its composition), the applied potential, and the electrolyte conditions.[22–28]

What is evident in mechanistic studies is that the rate-determining step (RDS) is the conversion of NO_3^- to NO_2^- (Figure 2A and B). In acidic media (Figure 2A), this step proceeds by following an electrochemical—chemical—electrochemical reaction (ECE*). Initially, NO_3^- is adsorbed and reduced to the dianion NO_3^{2-}. Subsequently, hydrolyzation of adsorbed NO_3^{2-} yields a nitrogen dioxide radical (NO_2•), and, eventually, NO_2• is reduced to NO_2^-. In alkaline media (Figure 2B), the RDS follows a similar pathway as in acidic media, but it is adjusted following the appropriate reduction steps.

Under highly acidic conditions and high NO_3^- concentrations (1.0 to 4.0 M NO_3^-), protonation of the adsorbed NO_2^- to nitrous acid (HNO_2) induces two autocatalytic mechanisms as proposed by Vetter and Schmid[29–33] (Figure 2C and D). When a sufficient amount of HNO_2 is present (>10^{-6} M), it dominates over NO_2^- leading to the spontaneous formation of several products, including nitric oxide (NO), nitrogen dioxide (NO_2), and HNO_2 as a result of disproportionation reactions.[30] According to the Vetter mechanism,[31] HNO_2 reacts with nitric acid (HNO_3) resulting in H_2O and a nitrogen dioxide dimer (N_2O_4) that is subsequently reduced into two NO_2 species. On the other hand, the Schmid mechanism[32,33] supports that NO^+ is the electrochemically active species that originates from the protonation of HNO_2. According to Schmid,[31] NO^+ is electrochemically reduced to NO and further converted to HNO_2. This either follows the proposed pathway by Schmid via N_2O_2 and H_2O or the HNO_3 and NO_{ads} reaction as proposed by Abel[34] (Figure 2E).

The previous pathways are preferred when NO_2^- is unstable. However, if $NO_2^-{}_{ads}$ is stable, it is electrochemically reduced to NO_{ads}, which opens an alternative reaction pathway to NH_3. These steps are influenced by the adsorption energy of NO_{ads} on the catalyst. A high adsorption energy results in catalyst poisoning while a low adsorption energy leads to the desorption of NO. In the case of NO_{ads} desorption, the literature suggests that N_2O and N_2 are the only products formed.[27,35] Vooys and Koper[36] support this through mechanistic studies with differential electrochemical mass spectrometry (DEMS), in which the reaction proceeds via dimerization of solvated NO and NO_{ads} via the Eley–Rideal mechanism (Figure 2F). The formed N_2O_2 gets protonated to HN_2O_2, which is then electrochemically reduced to N_2O_{ads} and H_2O. Further reduction to N_2 via N_2O is confirmed by Chumanov and coworkers (Figure 2F).[37]

Besides the formation of N_2 in acidic media, N_2 has also been detected in basic media.[38] Providing that NO desorption is prevented, the Duca—Feliu–Koper mechanism suggests the hydrogenation of NO_{ads} in a basic solution to $NH_{2,ads}$ (Figure 2G).[38] Subsequently, $NH_{2,ads}$ reacts with NO_{ads} and desorbs to form N_2 and H_2O. In weakly acidic conditions, Katsounaros and Kyriacou[39] propose an alternative surface reaction pathway according to the Langmuir–Hinshelwood mechanism (Figure 2H). NO_{ads} is protonated and potentially dimerizes into hyponitrous acid ($H_2N_2O_2$), which decomposes to N_2O and H_2O at ambient conditions. In the presence of HNO or HNO_2, Katsounaros and Kyriacou[39] also propose pathways for the formation of N_2 and N_2O from H_2NOH_{ads} (Figure 2I). The N_2O is believed to be the precursor of N_2, as proposed by Vooys and Koper.[35,40] Although not experimentally confirmed yet, an alternative route toward N_2 has been proposed via dimerization of N*. According to Chun and coworkers,[41] the energy barrier for the N_2 formation is higher than the hydrogenation of N*. Additional density functional theory (DFT) studies show that the migration barrier for N_{ads} lies higher than H_{ads}, which supports the favorable hydrogenation of N_{ads}.[42]

In addition the proposed pathways to N_2O and N_2, NO_{ads} can be reduced to hydroxylamine (NH_2OH) and NH_3 if desorption of NO_{ads} is prevented (Figure 2J).[28] Two direct electrocatalytic pathways are proposed for NH_3 synthesis (Figure 3)[35,39,43]. The first is direct electroreduction of NO_3^- [35,39] (Figure 3A), whereas the second pathway follows an H-assisted route, where H_2O is first reduced to result in H_{ads} (Figure 3B).[43] For the pathway

Mini Review
doi.org/10.1002/elsa.202100220
Chemistry Europe
European Chemical Societies Publishing

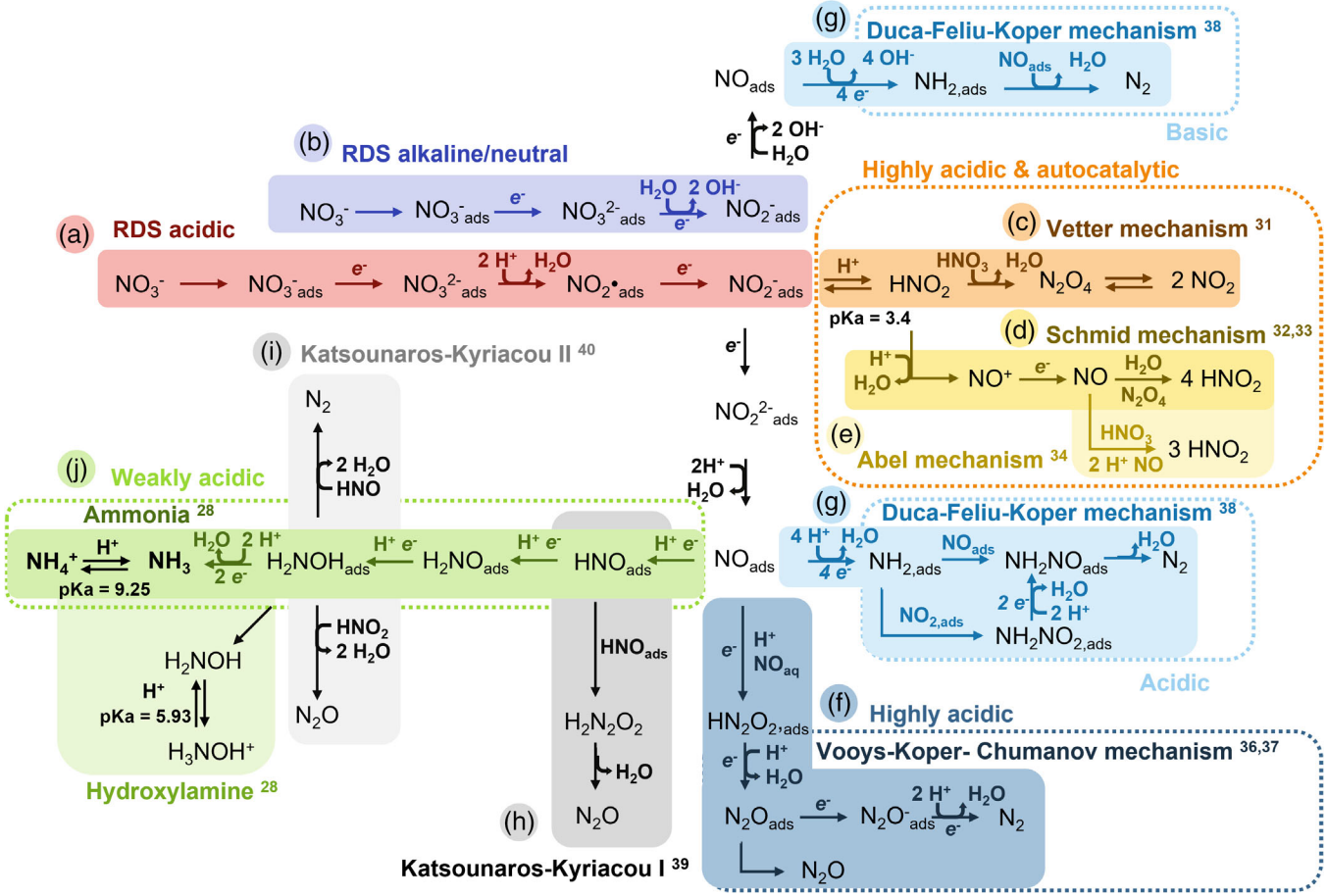

FIGURE 2 Overview of the proposed mechanisms for the electrochemical reduction of nitrate in aqueous media. Adapted from Ref. [15]. Copyright (2018) Applied Catalysis B: Environmental

following the direct electroreduction of NO_3^-, studies on Pt and Sn suggest the hydrogenation of NO_{ads} to HNO, H_2NO, H_2NOH, and eventually NH_3 (Figure 3C).[35,39] This pathway is supported by mechanistic studies on Cu-based catalysts, where NH_2OH was observed as a byproduct.[27,28,44] For the H-assisted pathway, hydrogen absorbs concurrently with NO_3^-, which is in turn stepwise reduced to NO_2^- and NO_{ads}.[43] Again, through concurrent adsorption of hydrogen, NO_{ads} is hydrogenated to form HNO_{ads}, H_2NO_{ads}, $NH_{2,ads}$, and finally NH_3 (Figure 3D). A recent study[43] on strained Ru clusters supported this mechanism by creating a reductive environment to form hydrogen radicals for the H-assisted electroreduction of NO_3^-.

Along with these two proposed pathways, the reaction conditions (e.g., concentration, pH, and potential) also have a strong influence on the reaction mechanism of electrochemical NO_3^- l reduction. Koper and coworkers[28] studied the mechanism of NO_3^- reduction on Cu(100) and Cu(111) surfaces in basic and acidic media using Fourier transform infrared spectroscopy. Their results show that the formation of NH_3 increases in acidic media while that of NO_2^- decreases. For basic conditions, the main product was NH_2OH, but NO_2^- appeared to be present as well, indicating a change in pathway depending on the pH of the bulk electrolyte. Furthermore, recent DFT studies[45,46] suggest different mechanistic pathways. Calculations on a Fe single-atom catalyst propose the hydrogenation of NO_3^- as the first step, followed by its reduction to NO_2^-, HNO_2, NO, and NH_3 (Figure 3E).[45] Another study on transition metals discussed that the formation of NOH_{ads} as a precursor is key for NH_3 production (Figure 3F).[46] The formation of NOH_{ads} proceeds via water-mediated hydrogenation of NO_{ads} since it has a lower activation barrier than the dissociation of NO_{ads}. A similar mechanism was found by Chen et al.[47] studying Cu-molecular solid catalysts (Figure 3G). Yao et al.[48] investigated the reaction intermediates in alkaline media with surface-enhanced infrared-absorption spectroscopy and DEMS on a Rh catalyst. N_2H_2 was observed in a low potential range (0.2 to -0.4 V vs. RHE) and suggested as an intermediate in NH_3 production. It was proposed that N_2H_2 decomposes into NH_3 and N_2. However, dissociation into N_2 and H_2 or further reduction cannot be ruled out.

Mini Review
doi.org/10.1002/elsa.202100220
Chemistry Europe
European Chemical Societies Publishing

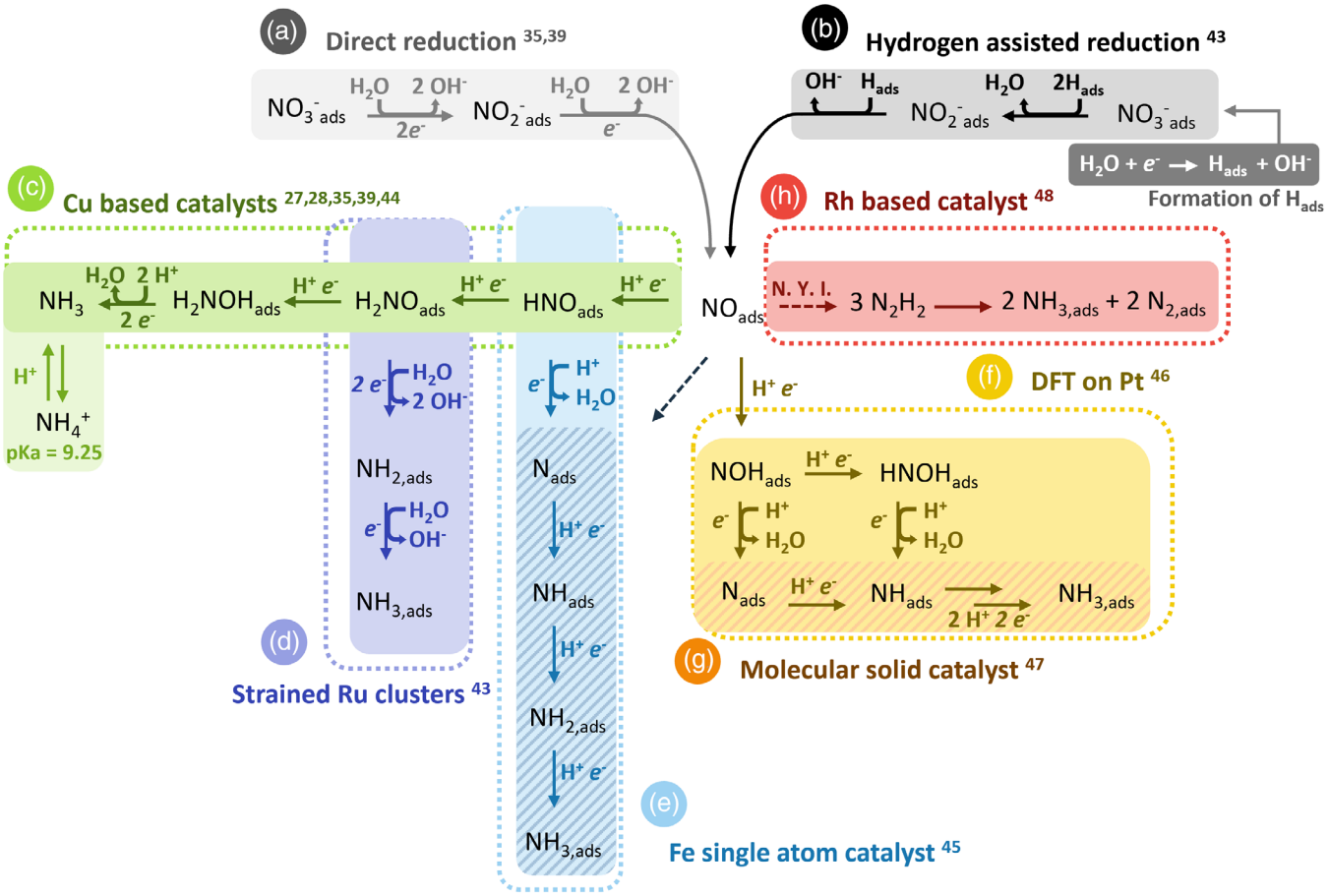

FIGURE 3 Mechanisms proposed by literature for ammonia synthesis from electrochemical nitrate reduction. N. Y. I. = not yet identified

Based on the above, it can be concluded that the adsorption energy of intermediate NO_{ads} is one of the critical parameters affecting the product distribution in electrochemicalNO_3^- reduction. Subsequent reduction of NO_{ads} is, therefore, believed to be the step that determines the selectivity.[49,50] Further theoretical studies on NO reduction on different metals indicated that the binding strength of NO* on the surface is a good descriptor to predict the reactivity of NO, one of the reaction intermediates in NO_3^- reduction.[51] Nevertheless, the applied potential should also be carefully taken into account as a parameter of influence in the product distribution, as demonstrated in a recent work from Rossmeisl et al.[52] Hence, the nature of the catalyst and the applied potential play an important role in determining selectivity.

3 | ELECTROCATALYSTS

Precious metal catalysts, such as Pt and Rh, have been commonly used to study NO_3^-RR to NH_3, focusing on the reaction mechanisms and kinetics concerning the adsorption of anions and hydrogen.[25,53–58] Even though Pt is not the most active metal for NO_3^- reduction, it has been studied the most for an in-depth understanding of the reaction mechanism.[25,53,55,58] Pt was chosen for NH_3 formation due to the high adsorption energy of the intermediate NO, consequently inhibiting solvation of NO, which is a precursor for N_2O and N_2. Studies on Pt single crystals by Dima et al.[53] showed that structure sensitivity plays an important role, mainly due to the adsorption of hydrogen and anions instead of NO_3^- adsorption, dissociation, or reduction. In a more recent study, Lim et al.[59] investigated the influence of the structure sensitivity of Pd on NO_3^- and NO_2^- reduction. The fabrication of shape-controlled nanoparticles shows that the presence of Pd(111) facets catalyze NO_3^- reduction at a higher rate than Pd(100) and Pd(*hk*0) (and for NO_2^- Pd[100] > Pd[*hk0*] > Pd[111]) in alkaline media. Cubooctahedrons that contain both Pd(100) and Pd(111) facets show the highest NH_3 production (306.8 μg/h/mg_{Pd}) (Figure 4). This bifunctional nature facilitates the side-by-side conversion of NO_3^- to NO_2^- on Pd(111) and NO_2^- to NH_3 on Pd(100), leading to a higher amount of NH_3.

Mini Review
doi.org/10.1002/elsa.202100220
Chemistry Europe
European Chemical Societies Publishing

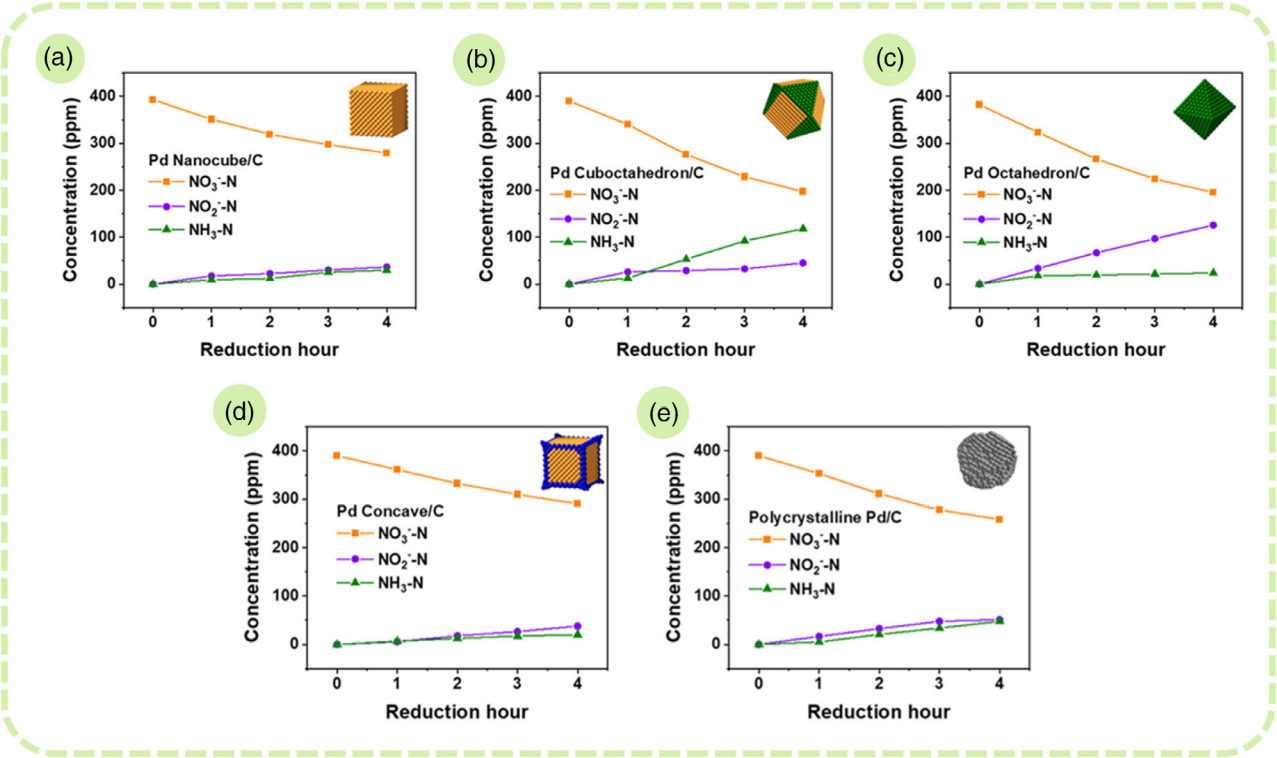

FIGURE 4 Concentration changes of NO_3—N, NO_2—N, and NH_3-N over reaction time during chronoamperometry tests using an H-cell at -0.2 V vs. RHE for (A) Pd nanocube/C, (B) Pd cuboctahedron/C, (C) Pd octahedron/C, (D) Pd concave/C, and (E) polycrystalline Pd/C. Reprinted with permission from Ref. [60]. Copyright 2021, American Chemical Society

Cu and Cu-based materials have also been extensively investigated for NO_3^-RR. The main interest in this metal is due to its low cost and high selectivity toward NH_3 in basic and neutral media.[28,44,47,60,61] Cu single crystal studies in alkaline media by Pérez-Gallent et al.[28] showed again evidence of NO_3^-RR being structure sensitive. The results showed that Cu(100) reduces NO_2^- with a higher rate than Cu(111), reaching almost negligible diffusion limitations. During the reduction, Cu(111) exhibited a higher deactivation of Cu(100). The authors suggested that the deactivation was caused by the formation of H_{ads} and increased hydrogen evolution reaction (HER) activity of the Cu(111) electrode. Fu et al.[60] reported corrosive behavior during NH_3 production on a Cu(111) nanosheet electrode. This was attributed to the formation of a soluble $Cu(NH_3)_2^+$ complex, resulting in corrosion of the electrocatalyst during electrolysis.[62] Nevertheless, the synthesized Cu(111) nanosheets produced NH_3 with a low overpotential (-0.15 V vs. RHE in 0.1 M KOH) and a FE of 99.7%.[60] The critical role of oxygen vacancy defects (with one free electron) within CuO nanomaterials for NO_3^-RR was reported by Daiyan et al.[63] In combination with DFT calculations they revealed that the presence of oxygen vacancies (OVs) can lead to the adsorption of NO_3^- intermediates. They reported a direct correlation of oxygen vacancy density with NH_4^+ yield and a maximum faradaic efficiency of 89%. CuO nanowire arrays (NWAs) were also tested for NO_3^- reduction with a reported FE of 95.8% for NH_3.[61] Using in situ Raman, the authors showed that CuO was electrochemically converted to Cu/Cu_2O NWAs, suggesting that latter are the active phases. It was suggested that Cu/Cu_2O NWAs lower the energy for *NOH formation due to an increased electron density and subsequently suppress HER.

A Cu-molecular solid catalyst, Cu-3,4,9,10-perylene tetracarboxylic dianhydride (Cu-PTCDA), was synthesized and showed a unique electronic structure of Cu. This structure could suppress HER and simultaneously boost H–N bond formation through proton and electron transfer between PTCDA and the Cu active site. The maximum FE reached was 85.9% at −0.4 V versus RHE in a neutral medium after 4 h. This result was attributed first to the highly occupied d-orbital of the Cu-based active center accommodating the charge injection to the LUMO of NO_3^- and, second, to the presence of PTCDA.[47] Others studies on Cu-based molecular catalysts indicated similar performance, suggesting that the activity originated from the Cu active site and that there were no contributions of the PTCDA structure.[60,61]

Besides the large interest in Cu-based catalysts, Co has attracted attention from researchers as well.[22,64,65] Investigations on cobalt molecular solid catalysts showed

promising results for NH_3 production on Co-PTCDA with a FE of 62.9%.[47] Deng et al.[64] also reported the use of metallic Co, synthesized as Co nanoarrays (NAs), to catalyze NH_3 production at high current densities (>2 A/cm^2). The Co NAs proved to be HER-inert, which makes them interesting electrocatalysts for NH_3 synthesis. In addition, a wide operational potential range was reported (0.11 to -0.24 V vs. RHE in 1 M KOH) with FEs close to 100%. Moreover, the stability of the Co NAs was promising since only a mild structural degradation was observed with scanning electron microscopy and a FE of 98% was maintained for 10 h during electrolysis.[64] Yu et al.[22] developed nanostructured Co electrocatalysts via electrodeposition of $Co(OH)_2$ onto Ni foam followed by calcination to CoO, Co/CoO, and Co nanosheet arrays (NSAs). High FE (93.8%) and selectivity (91.2%) toward NH_3 were observed for mixed metal–metal oxide Co/CoO NSAs. It was suggested that the increased catalytic performance was a consequence of electron deficiency of Co induced by the rectifying Schottky contact in the mixed metal–metal oxide structures. It was suggested that the electron transfer at the interphase of Co and CoO suppressed HER and increased the energy barrier for byproducts. The most recent study on Co-based catalysts included CoP nanorings, which showed good activity toward HER and NO_3^-RR.[66] A FE of 97.1% toward NH_3 ($yield_{NH3}$ = 30.1 mg/ h/mg_{cat}) was achieved in neutral media at -0.5 V versus RHE. The improved activity of the nanorings was attributed to their morphology which included a lot of high-indexed facets and coordinately unsaturated active sites.

Further studies included the investigation of Ti as an electrocatalyst material due to its high corrosion resistance, poor HER activity, large operating window, abundance, and low cost.[67,68] McEnaney et al.[67] studied the impact of electrochemical conditions such as pH, NO_3^- concentration, and applied potential on a Ti electrode. A high concentration of protons and NO_3^- was necessary to achieve a high selectivity toward ammonia with a FE of 82% (-1 V vs. RHE and -22 mA/cm^2). Besides metallic Ti, TiO_2 is a feasible electrocatalyst through the introduction of OVs.[68] An NH_3 yield of 0.045 mmol/h/mg was reported with a selectivity of 87.1% toward NH_3. Both the catalyst and production rate proved to be stable for eight cycles of 2 h. However, for it to be applicable in industry, the stability and selectivity of these catalysts must be improved.[69]

Poor stability and high material costs have led to the investigation of bimetallics and alloys as well as modified electrocatalysts by the addition of dopants or surface modifiers. The addition of a second metal or dopant can lead to electronic effects (e.g., strain effect or a shift in d-band energy), third body effects, or bifunctional effects. These effects can help to tune the adsorption energy of reaction intermediates, the pathway of the reaction, and the formation rate of the desired product while suppressing byproducts and side-reactions. Studies on Pt focused on Pt(100) surface and its modification via adatoms.[38,70–72] The results of these studies showed that Pt(100) can lead to different products depending on the reaction medium: alkaline media promoted the production of N_2, whereas acidic solutions led to the preferential formation of NH_3.[71,72] When this surface was modified by Cu or Sn adatoms, the electrode showed no NH_3 production but N_2 or N_2O instead.[70,71] In alkaline media, only Rh-Pt(100) electrodes resulted in the formation of NH_3.[72] Li et al.[43] used oxygen dopants to develop strained Ru nanoclusters and reported a FE of NH_3 of almost 100% with current densities higher than 120 mA/cm^2. The catalyst showed good stability over 100 h. Its stability was attributed to subsurface Ru−O coordination and the high NH_3 selectivity to the strains induced from the oxygen dopant to the Ru unit cell.[43] The authors argued that such strain suppressed HER but favored hydrogen radical formation by lifting the barrier of hydrogen−hydrogen coupling. Finally, the hydrogenation of reaction intermediates to NH_3 was promoted via the resulting hydrogen radical (H•). Using 5,5-dimethyl-1-pyrroline-N-oxide (DMPO) to trap the hydrogen radical, the effect of the strain-dependent NO_3^- reduction reaction performance can be visualized (Figure 5A).

Alteration of the surface composition through alloying has also been used to improve efficiency and selectivity toward NH_3 production from NO_3^-. Preliminary studies focused on the use of bimetallic electrodes based on palladium including Cu-Pd, Ag-Pd, Ni-Pd, and Rh-Pd.[73–77] These all showed an acceptable selectivity toward NH_3, however, only Rh-Pd showed adequate NO_2^- reduction rates, yielding 75% NH_3. On Cu-Ni alloys,[78,79] an effect of the Cu-Ni ratio was found. Mattarozzi et al.[79] showed that the Cu-rich alloys have a selectivity of 88% toward NH_3 from NO_3^- and an even higher selectivity of 96% for NO_2^- electroreduction (both at a reduction potential of -1.2 V vs. Hg/HgO for 4 h). Based on upshifts observed in UV photoelectron spectroscopy (UPS), Wang et al.[78] explained this effect with changes in the bandgap of the Fermi level induced by the different Cu-Ni ratios. This led to a decrease in the antibonding occupation in the absorbed reactant. Hence, the adsorption energy of the intermediate species increased for Cu_{30}-Ni_{70} (Figure 5B). This affected the RDS, resulting in an improved selectivity toward NH_3 for the Cu-rich alloys. Additionally, an 0.12 V versus RHE (pH = 14) increase in the half-wave potential was suggested to be a descriptor for improved catalytic activity. The overpotential required for NH_3 was also lowered by 0.2 V, indicating the improved performance of the Cu-Ni catalyst.[78]

Other studies focused on the electroanalysis of porous Cu-based catalysts, decorating the surface through electrodeposition of Cu-Ni or galvanic exchange of Rh and Cu

Mini Review
doi.org/10.1002/elsa.202100220
Chemistry Europe
European Chemical Societies Publishing

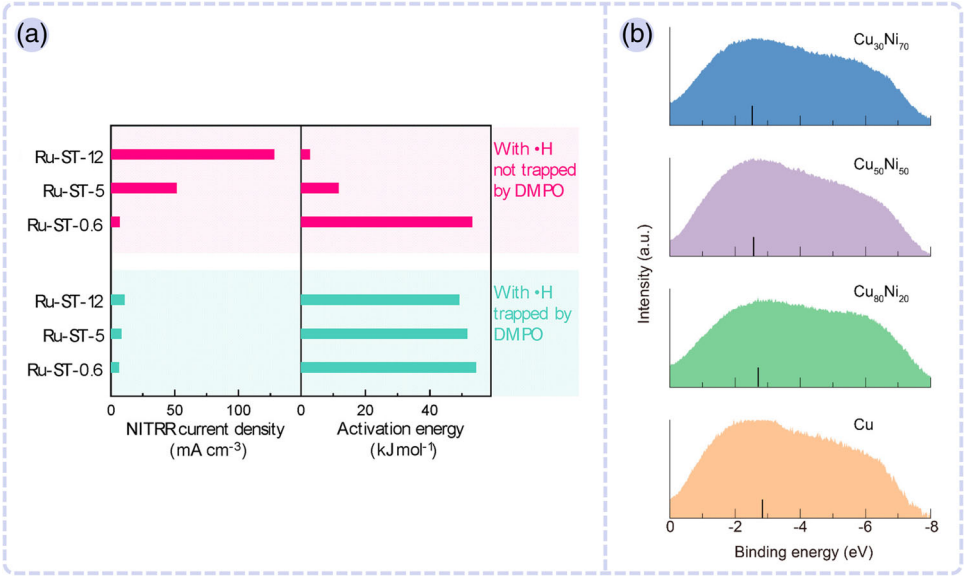

FIGURE 5 (a) Nitrate reduction reaction partial current densities and activation energies of Ru-ST-12, Ru-ST-5, and Ru-ST-0.6 with and without DMPO involvement. (b) UPS spectra and d-band center positions of pure Cu catalysts and CuNi alloys. Reprinted with permission from Refs. [43] and [78]. Copyright 2021, American Chemical Society

to obtain Rh-modified Cu electrodes.[80] The porous Cu-Ni proved most stable, whereas the Rh-modified Cu showed a significant enhancement of NO_3^- and NO_2^- electroreduction, which in turn seemed promising for further investigation. Binder-less Fe-Ni alloy nanoparticles on graphitized mesoporous carbon on Ni foam (Fe-Ni/g-mesoC/NF, 7.3 wt.% Fe) were fabricated to improve the stability of the electrocatalyst.[81] Fe has a high NO_3^- removal efficiency and Ni is thermodynamically stable over a larger potential range and active for NO_2^- hydrogenation.[79] The fabricated Fe-Ni/g-mesoC/NF composite electrode showed enhanced catalytic activity, which is introduced by the micro-/nanostructure with OVs in the passivation layers.[81] The NH_3 selectivity was 80% and the catalyst was stable over 30 cycles over 1 month. It must be noted that 0.03 wt.% of Fe leached in 24 h, which eventually resulted in reduced performance over time. Nevertheless, the subsurface OVs appeared to be stable and were regenerated during the electrocatalytic reduction according to their XPS spectra before and after the reaction.

Figure 6 shows an overview of the Faradaic efficiency toward NH_3^- (FE_{NH3}) and the total current density reached for the catalysts discussed in this review. The correlations are plotted with respect to the Ag/AgCl potential scale to provide a catalyst comparison independent of the solution's pH. From Figure 6A, it is apparent that, besides the nature of the catalyst, the applied potential plays a significant role in the $FE_{NH3.}$ Unfortunately, most of the studies focus on the quantification of particular products, omitting a full analysis of the products. Therefore, no conclusions can be made on the electrochemical potential effect on the

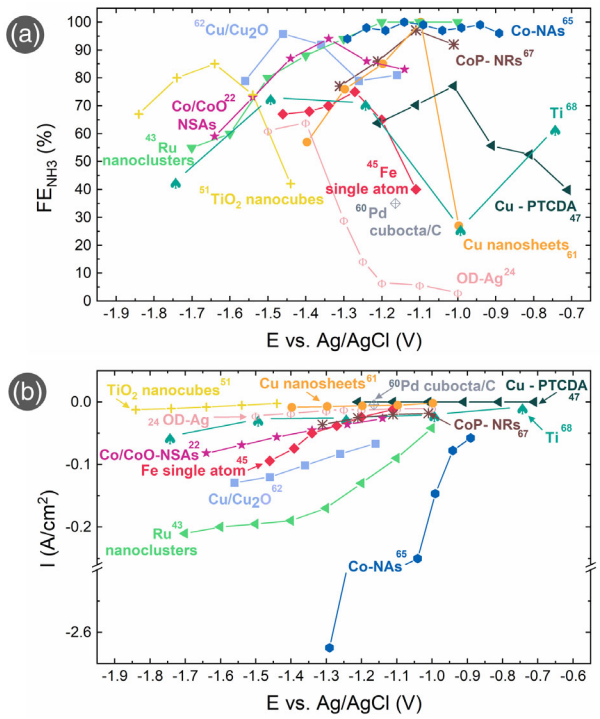

FIGURE 6 (A) Overview of the Faradaic efficiency of NO_3^- electroreduction to NH_3, FE_{NH3} (%) at different applied potentials, E vs. Ag/AgCl (V). (B) Overview of the total current density, I (mA/cm^2) of NO_3^- electroreduction at different applied potentials, E versus Ag/AgCl (V)

product distribution based on these data. The majority of the catalysts in Figure 6A show a high FE_{NH3} (>80%) but only a few reach these values at low overpotential (> -1.0

V versus RHE). In addition to the high overpotential, the majority of the catalysts studied so far showed a total current density below 100 mA/cm^2 (Figure 6B). However, the Ru nanoclusters[43] showed a current density higher than 200 mA/cm^2 but at potentials where H_2 evolution is prominent. Co NAs[64] seem to be the best-performing catalyst because they showed a significantly higher current density at low overpotential, while obtaining a FE_{NH3} above 90%. To conclude, even though a significant advancement has been made in terms of FE_{NH3} from NO_3^-, the rate and selectivity of the reaction are still low. Studies that include the overall product distribution are still scarce, and reported FE_{NH3} on bimetallics are missing. Finally, the stability of the catalysts studied so far is another important aspect yet to be evaluated.

4 | CONCLUSIONS AND OUTLOOK

Besides the clear importance of NH_3 in the agricultural industry, NH_3 has the potential to become one of the central molecules of future energy as a dense energy carrier.[3] Its carbon-free nature, high energy density, and established infrastructure make it an excellent candidate for the replacement of fuel from hydrocarbons. This review summarized the most recent advances in the field of NO_3^- electroreduction from diluted aqueous solutions (wastewater) with an emphasis on potential electrocatalyst to produce NH_3. Aqueous NO_3^- solutions are of high fundamental interest to understand the catalysis and reaction mechanisms. However, due to low NO_3^- concentrations, such a process would only produce low amounts of NH_3. For an efficient electrochemical NH_3 production from NO_3^-, a more concentrated source of NO_3^-, such as NO_3^-/NO_2^- derived from air plasma activation, can be explored.[82,83] Despite the recent advances in the NO_3^- electroreduction reaction, no reported system is yet viable. Significant improvements are needed to make a step toward implementing such technology at a larger scale. In terms of catalyst development, noble metals show high performance for NO_3^- reduction, but their high cost is daunting to consider for industrial applications.[84] Other materials, like bimetallics or alloys, are being developed as a potential solution to this challenge.[78,85] To successfully advance these materials, the synergistic work of in situ surface science investigations is required. An in-depth understanding of the catalyst behavior under reaction conditions will help tackle challenges like catalyst dissolution and stabilization, which are aspects that require further attention. In addition, other catalyst examples can be obtained from different research areas as a source of inspiration like the addition of ligands or dopants.[86,87] Looking at the current research of NO_3^- reduction and its mechanisms, attention should be paid to the adsorption strength of NO and H_{ads} when developing a catalyst.[88] It has been proven that catalysts with high adsorption strength for hydrogen limit the conversion rate of NO_3^- due to the unavailability of active sites. On the contrary, the HER takes over when the H adsorption is too low. The binding strength of the reaction intermediates can be controlled by changing the local electronic structure of the catalyst surface. This can be controlled with oxide-derived materials by tuning the surface oxidation state,[24] or with alloys, since surface interactions between two different elements can change their electronic state and chemical properties. Catalyst structure and morphology are additional factors that can be adjusted to improve catalytic activity and selectivity toward the desired product.[53,59,89] Grain boundaries, edges, and steps can result in significantly different adsorption energies and interactions with reactants and intermediates. So far, there is limited research on the impact of particle size, shape, exposed facets, and defects of nanomaterials (e.g., atom vacancies) but in the past couple of years, more studies are emerging.[63,89] In situ characterization and visualization of catalysts under working conditions accompanied by theoretical simulations can also add valuable information on the topic. They would provide insights on how to modify the catalyst structure to regulate strengths between the active intermediates and the catalyst sites. Aspects, such as thermodynamics, kinetics, and infrastructure must be deeply understood and optimized. Undoubtedly, there are still a lot of opportunities to further optimize this reaction. The works cited show the efforts that the electrochemical community is putting into understanding the NO_3^- reduction reaction as such, and certainly in the context of NH_3 production. The main key advances to arrive at the current stage from the catalyst perspective were formulated in this work.

ACKNOWLEDGMENTS

The authors acknowledge the financial support of the Eindhoven Institute of renewable energy systems (EIRES) and the Strategic Alliance TU/e-UU-WUR.

CONFLICT OF INTEREST

The authors declare no conflict of interest.

DATA AVAILABILITY STATEMENT

Data derived from public domain resources.

REFERENCES

1. G. Qing, R. Ghazfar, S. T. Jackowski, F. Habibzadeh, M. M. Ashtiani, C. P. Chen, M. R. Smith, T. W. Hamann, *Chem. Rev.* **2020**, *120*, 5437.
2. S. Giddey, S. P. S. Badwal, C. Munnings, *Chem. Eng.* **2017**, *5* (11), 10231.

3. The Royal Society (2020). Fuel and energy store. Policy briefing. **2020**.
4. C. Zamfirescu, I. Dincer, *J. Power Sources* **2008**, *185*, 459.
5. O. Elishav, B. Mosevitzky Lis, A. Valera-Medina, G. S. Grader, *Techno-Economic Challenges of Green Ammonia as an Energy Vector*. Academic Press, MA, **2021**, p. 85. https://doi.org/10.1016/b978-0-12-820560-0.00005-9
6. D. R. MacFarlane, P. V. Cherepanov, J. Choi, B. H. R. Suryanto, R. Y. Hodgetts, J. M. Bakker, F. M. Ferrero Vallana, A. N. Simonov, *Joule* **2020**, *4*, 1186.
7. D. Erdemir, I. Dincer, *Int. J. Energy Res.* **2021**, *45*, 4827.
8. V. Pattabathula, J. Richardson, Introduction to Ammonia Production | AIChE. (Accessed September 15, 2021).
9. M. Wang, M. A. Khan, I. Mohsin, J. Wicks, A. H. Ip, K. Z. Sumon, C.-T. Dinh, E. H. Sargent, I. D. Gates, M. G. Kibria, *Energy Environ. Sci.* **2021**, *14*, 2535.
10. P. H. van Langevelde, I. Katsounaros, M. T. M. Koper, *Joule* **2021**, *5*, 290.
11. A. R. Singh, B. A. Rohr, J. A. Schwalbe, M. Cargnello, K. Chan, T. F. Jaramillo, I. Chorkendorff, J. K. Nørskov, *ACS Catal.* **2017**, *7*, 706.
12. J. Lim, C. A. Fernández, S. W. Lee, M. C. Hatzell, *ACS Energy Lett.* **2021**, *6*, 3676.
13. D. Hao, Z. G. Chen, M. Figiela, I. Stepniak, W. Wei, B. J. Ni, *J. Mater Sci. Technol*. **2021**, *77*, 163.
14. S. K. M. Huno, E. R. Rene, E. D. Van Hullebusch, A. P. Annachhatre, *J. Water Supply Res. Technol.- AQUA* **2018**, *67*, 885.
15. S. Garcia-Segura, M. Lanzarini-Lopes, K. Hristovski, P. Westerhoff, *Appl. Catal., B*. **2018**, *236*, 546.
16. X. Zhang, E. A. Davidson, D. L. Mauzerall, T. D. Searchinger, P. Dumas, Y. Shen, *Nature* **2015**, *528*, 51.
17. World Health Organization. *Guidelines for Drinking-Water Quality: Fourth Edition Incorporating the First Addendum*, **2014**.
18. Ö. Bodin, M. Tengö, A. Norman, J. Lundberg, T. Elmqvist, S. Lansing, J. Norberg, *Ecol. Appl.* **2006**, *16*, 440.
19. A. Kapoor, T. Viraraghavan, *J. Environ. Eng.* **1997**, *123*, 371.
20. A. Matei, G. Racoviteanu, *IOP Conf. Ser. Earth Environ. Sci.* **2021**, *664*, 012024.
21. A. J. Bard, R. Parsons, J. Jordan, *Standard Potentials in Aqueous Solution*, M. Dekker, New York **2017**. https://doi.org/10.1201/9780203738764
22. Y. Yu, C. Wang, Y. Yu, Y. Wang, B. Zhang, *Sci. China Chem.* **2020**, *63*, 1469.
23. T. Favarini Beltrame, M. C. Gomes, L. Marder, F. A. Marchesini, M. A. Ulla, A. Moura Bernardes, *J. Water Process Eng.* **2020**, *35*, 101189.
24. H. Liu, J. Park, Y. Chen, Y. Qiu, Y. Cheng, K. Srivastava, S. Gu, B. H. Shanks, L. T. Roling, W. Li, *ACS Catal.* **2021**, *16*, 8431.
25. M. T. De Groot, M. T. M. Koper, *J. Electroanal. Chem.* **2004**, *562*, 81.
26. J. Yang, F. Calle-Vallejo, M. Duca, M. T. M. Koper, *Chem. Cat. Chem.* **2013**, *5*, 1773.
27. G. E. Dima, A. C. A. De Vooys, M. T. M. Koper, *J. Electroanal. Chem.* **2003**, *554–555*, 15.
28. E. Pérez-Gallent, M. C. Figueiredo, I. Katsounaros, M. T. M. Koper, *Electrochim. Acta.* **2017**, *227*, 77.
29. R. Lange, E. Maisonhaute, R. Robin, V. Vivier, *Electrochem. Commun.* **2013**, *29*, 25.
30. I. Katsounaros, *Curr. Opin. Electrochem.* **2021**, *28*, 100721.
31. K. J. Vetter, *Zeitschrift für Elektrochemie, Berichte der Bunsengesellschaft für Phys. Chemie* **1959**, *63*, 1189.
32. G. Schmid, D. Jochen, Die Autokatalytische Natur Der Kathodischen Reduktion von Salpetersaure Zu Salpetriger Siiure II. Der Galvanostatische Einschaltvorgang. **1959**, 1192.
33. G. Schmid, Die AutokatalytischeDie Autokatalytische Natur Der Kathodischen Reduktion Yon Salpetersiiure Zu Salpetriger Shre III. Mathematische Behandlung Einer Autokatalytischen Elektrodenreaktion 1. Ordnung. **1961**, *4*, 531–534.
34. E. Abel, H. Schmid, *Zeitschrift für Phys. Chemie* **1928**, *136U*, 430.
35. A. C. A. de Vooys, G. L. Beltramo, B. van Riet, J. A. R. van Veen, M. T. M. Koper, *Electrochim. Acta.* **2004**, *49*, 1307.
36. A. C. de Vooys, M. T. Koper, R. van Santen, J. A. van Veen, *J. Catal.* **2001**, *202*, 387.
37. J. Zheng, T. Lu, T. M. Cotton, G. Chumanov, *J. Phys. Chem. B* **1999**, *103*, 6567.
38. M. Duca, M. C. Figueiredo, V. Climent, P. Rodriguez, J. M. Feliu, M. T. M. Koper, *J. Am. Chem. Soc.* **2011**, *133*, 10928.
39. I. Katsounaros, G. Kyriacou, *Electrochim. Acta* **2008**, *53*, 5477.
40. F. Zaera, C. S. Gopinath, *Chem. Phys. Lett.* **2000**, *332*, 209.
41. H. J. Chun, V. Apaja, A. Clayborne, K. Honkala, J. Greeley, *ACS Catal.* **2017**, *7*, 3869.
42. H. Shin, S. Jung, S. Bae, W. Lee, H. Kim, *Environ. Sci. Technol.* **2014**, *48*, 12768.
43. J. Li, G. Zhan, J. Yang, F. Quan, C. Mao, Y. Liu, B. Wang, F. Lei, L. Li, A. W. M. Chan, L. Xu, Y. Shi, Y. Du, W. Hao, P. K. Wong, J. Wang, S.-X. Dou, L. Zhang, J. C. Yu, *J. Am. Chem. Soc.* **2020**, *142*, 7036.
44. D. Reyter, D. Bélanger, L. Roué, *Electrochim. Acta* **2008**, *53*, 5977.
45. Z. Y. Wu, M. Karamad, X. Yong, Q. Huang, D. A. Cullen, P. Zhu, C. Xia, Q. Xiao, M. Shakouri, F. Y. Chen, J. Y. T. Kim, Y. Xia, K. Heck, Y. Hu, M. S. Wong, Q. Li, I. Gates, S. Siahrostami, H. Wang, *Nat. Commun.* **2021**, *12*, 2870.
46. C. A. Casey-Stevens, H. Ásmundsson, E. Skúlason, A. L. Garden, *Appl. Surf. Sci.* **2021**, *552*.
47. G. F. Chen, Y. Yuan, H. Jiang, S. Y. Ren, L. X. Ding, L. Ma, T. Wu, J. Lu, H. Wang, *Nat. Energy* **2020**, *5*, 605.
48. Y. Yao, S. Zhu, H. Wang, H. Li, M. Shao, *Angew. Chemie* **2020**, *132*, 10565.
49. M. Duca, M. T. M. Koper, *Energy Environ. Sci.* **2012**, *5*, 9726.
50. Z. Wang, D. Richards, N. Singh, *Catal. Sci. Technol.* **2021**, *11*, 705.
51. H. J. Chun, Z. Zeng, J. Greeley, *ACS Catal.* **2022**, *12*, 1394.
52. H. Wan, A. Bagger, J. Rossmeisl, *Angew. Chemie-Int. Ed.* **2021**, *60*, 21966.
53. G. E. Dima, G. L. Beltramo, M. T. M. Koper, *Electrochim. Acta* **2005**, *50*, 4318.
54. V. Rosca, M. Duca, M. T. De Groot, M. T. M. Koper, *Chem. Rev.* **2009**, *109*, 2209.
55. E. B. Molodkina, I. G. Botryakova, A. I. Danilov, J. Souza-Garcia, J. M. Feliu, *Russ. J. Electrochem.* **2012**, *48*, 302.
56. M. Duca, B. Van Der Klugt, M. A. Hasnat, M. MacHida, M. T. M. Koper, *J. Catal.* **2010**, *275*, 61.
57. W. Siriwatcharapiboon, Y. Kwon, J. Yang, R. L. Chantry, Z. Li, S. L. Horswell, M. T. M. Koper, *Chem. ElectroChem.* **2014**, *1*, 172.
58. M. C. Figueiredo, J. Solla-Gullón, F. J. Vidal-Iglesias, V. Climent, J. M. Feliu, *Catal. Today* **2013**, *202*, 2.
59. J. Lim, C.-Y. Liu, J. Park, Y.-H. Liu, T. P. Senftle, S. W. Lee, M. C. Hatzell, *ACS Catal.* **2021**, *11*, 7568.

60. X. Fu, X. Zhao, X. Hu, K. He, Y. Yu, T. Li, Q. Tu, X. Qian, Q. Yue, M. R. Wasielewski, Y. Kang, *Appl. Mater. Today* **2020**, *19*, 100620.
61. Y. Wang, W. Zhou, R. Jia, Y. Yu, B. Zhang, *Angew. Chem., Int. Ed.* **2020**, *59*, 5350.
62. A. C. A. De Vooys, M. T. M. Koper, R. A. Van Santen, J. A. R. Van Veen, *J. Electroanal. Chem.* **2001**, *506*, 127.
63. R. Daiyan, T. Tran-Phu, P. Kumar, K. Iputera, Z. Tong, J. Leverett, M. H. A. Khan, A. Asghar Esmailpour, A. Jalili, M. Lim, A. Tricoli, R.-S. Liu, X. Lu, E. Lovell, R. Amal, *Energy Environ. Sci.* **2021**, *14*, 3588.
64. X. Deng, Y. Yang, L. Wang, X. Z. Fu, J. L. Luo, *Adv. Sci.* **2021**, *8*, 1.
65. W. Ye, W. Zhang, X. Hu, S. Yang, W. Liang, *Sci. Total Environ.* **2020**, *732*, 139245.
66. Q.-L. Hong, J. Zhou, Q.-G. Zhai, Y.-C. Jiang, M.-C. Hu, X. Xiao, S.-N. Li, Y. Chen, *Chem. Commun.* **2021**, *57*, 11621.
67. J. M. McEnaney, S. J. Blair, A. C. Nielander, J. A. Schwalbe, D. M. Koshy, M. Cargnello, T. F. Jaramillo, *ACS Sustainable Chem. Eng.* **2020**, *8*, 2672.
68. R. Jia, Y. Wang, C. Wang, Y. Ling, Y. Yu, B. Zhang, *ACS Catal.* **2020**, *10*, 3533.
69. C. J. Werth, C. Yan, J. P. Troutman, *ACS ES&T Eng*. **2020**, *1*, 6.
70. E. B. Molodkina, I. G. Botryakova, A. I. Danilov, J. Souza-Garcia, J. M. Feliu, *Russ. J. Electrochem.* **2013**, *49*, 285.
71. J. Yang, M. Duca, K. J. P. Schouten, M. T. M. Koper, *J. Electroanal. Chem.* **2011**, *662*, 87.
72. T. Chen, H. Li, H. Ma, M. T. M. Koper, *Langmuir.* **2015**, *31*, 3277.
73. M. A. Hasnat, M. R. Karim, M. Machida, *Catal. Commun.* **2009**, *10*, 1975.
74. A. Anastasopoulos, L. Hannah, B. E. Hayden, *J. Catal.* **2013**, *305*, 27.
75. K. A. Guy, H. Xu, J. C. Yang, C. J. Werth, J. R. Shapley, *J. Phys. Chem. C* **2009**, *113*, 8177.
76. A. C. A. De Vooys, R. A. Van Santen, J. A. R. Van Veen, *J. Mol. Catal. A: Chem.* **2000**, *154*, 203.
77. L. Mattarozzi, S. Cattarin, N. Comisso, R. Gerbasi, P. Guerriero, M. Musiani, E. Verlato, *Electrochim. Acta.* **2017**, *230*, 365.
78. Y. Wang, A. Xu, Z. Wang, L. Huang, J. Li, F. Li, J. Wicks, M. Luo, D. H. Nam, C. S. Tan, Y. Ding, J. Wu, Y. Lum, C.-T. Dinh, D. Sinton, G. Zheng, E. H. Sargent, *J. Am. Chem. Soc.* **2020**, *142*, 5702.
79. L. Mattarozzi, S. Cattarin, N. Comisso, P. Guerriero, M. Musiani, L. Vázquez-Gómez, E. Verlato, *Electrochim. Acta.* **2013**, *89*, 488.
80. N. Comisso, S. Cattarin, P. Guerriero, L. Mattarozzi, M. Musiani, L. Vázquez-Gómez, *J. Solid State Electrochem.* **2016**, *20*, 1139.
81. X. Chen, T. Zhang, M. Kan, D. Song, J. Jia, Y. Zhao, X. Qian, *Environ. Sci. Technol.* **2020**, *54*.
82. J. Sun, D. Alam, R. Daiyan, H. Masood, T. Zhang, R. Zhou, P. J. Cullen, E. C. Lovell, A. Jalili, R. Amal, *Energy Environ. Sci.* **2021**, *14*, 865.
83. L. Li, C. Tang, X. Cui, Y. Zheng, X. Wang, H. Xu, S. Zhang, T. Shao, K. Davey, S. Z. Qiao, *Angew. Chemie-Int. Ed.* **2021**, *60*, 14131.
84. M. C. Figueiredo, I. Katsounaros, *Encycl. Interfacial Chem. Surf. Sci. Electrochem.* **2018**, 761-768. https://doi.org/10.1016/B978-0-12-409547-2.13347-5
85. N. Comisso, S. Cattarin, S. Fiameni, R. Gerbasi, L. Mattarozzi, M. Musiani, L. Vázquez-Gómez, E. Verlato, *Electrochem. Commun.* **2012**, *25*, 91.
86. Q. J. Bruch, G. P. Connor, N. D. McMillion, A. S. Goldman, F. Hasanayn, P. L. Holland, A. J. M. Miller, *ACS Catal.* **2020**, *10*, 10826.
87. Y. Huo, X. Peng, X. Liu, H. Li, J. Luo, *ACS Appl. Mater. Interfaces* **2018**, *10*, 12618.
88. Y. Wang, C. Wang, M. Li, Y. Yu, B. Zhang, *Chem. Soc. Rev.* **2021**, *50*, 6720.
89. R. M. Arán-Ais, F. Scholten, S. Kunze, R. Rizo, B. Roldan Cuenya, *Nat. Energy* **2020**, *5*, 317.

How to cite this article: D. Anastasiadou, Y. van Beek, E. J. M. Hensen, M. Costa Figueiredo. *Electrochem Sci Adv.* **2023**, *3,* e2100220. https://doi.org/10.1002/elsa.202100220